BMJ Open Ophthalmology

Characterisation of vascular changes in different stages of Stargardt disease using double swept-source optical coherence tomography angiography

Michael Reich , Andreas Glatz, Bertan Cakir, Daniel Böhringer, Stefan Lang, Sebastian Küchlin, Lutz Joachimsen, Wolf Lagreze, Hansjuergen T Agostini, Clemens Lange

To cite: Reich M, Glatz A, Cakir B, *et al*. Characterisation of vascular changes in different stages of Stargardt disease using double swept-source optical coherence tomography angiography. *BMJ Open Ophthalmology* 2019;**4**:e000318. doi:10.1136/bmjophth-2019-000318

Received 9 April 2019
Revised 2 September 2019
Accepted 13 October 2019

Eye Center, Medical Center, Faculty of Medicine, University of Freiburg, Freiburg, Germany

Correspondence to
Dr Clemens Lange; clemens.lange@uniklinik-freiburg.de

ABSTRACT

Objective To describe vascular changes in different stages of Stargardt disease (STGD) via double swept-source optical coherence tomography angiography.

Methods and analysis Prospective, cross-sectional case–control study. Twenty-three patients (45 eyes) with ABCA4 mutations graded according to the Fishman STGD classification and 23 controls (23 eyes) were included. Two independent investigators quantified the foveal avascular zone (FAZ) in the superficial and deep capillary plexus (SCP/DCP) and the areas presenting rarefied flow and complete vascular atrophy in the outer retina to choriocapillaris (ORCC) and choriocapillaris (CC) slab.

Results The mean age at first diagnosis of STGD was 24.0 years (range 9–50) and 37.9 years (range 18–74) at the time of examination. Eleven patients were assigned to the Fishman STGD classification stage (S) 1, three to S2, eight to S3 and one to S4. The FAZ in SCP and DCP was increased in all stages compared with controls ($p<0.01$). Areas with rarefied flow signal and vascular atrophy were detected in the ORCC and the CC layer and grew with increasing stage of disease ($p<0.01$). The duration of disease correlated with the extent of the enlarged FAZ in the SCP/DCP and with the area of reduced flow in the ORCC and CC layer ($p<0.01$). Best corrected visual acuity correlated negatively with the extent of the enlarged FAZ in the SCP/DCP ($p<0.0001$), as well as with enlarged atrophic area in the ORCC and CC layer ($p=0.026$ and $p=0.074$).

Conclusions Patients with STGD reveal vascular changes in the retina and CC in all disease stages. The avascular zone in the SCP/DCP and areas with rarefied flow signal in the ORCC/CC increase with the duration and stage of disease, indicating progressive vascular decay most likely secondary to retinal pigment epithelium and neuronal loss. Furthermore, increased vascular damage is associated with decreased vision.

key message

What is already known about this subject?

- Stargardt disease (STGD) is associated with vascular alterations in the retina and choroid as shown by optical coherence tomography (OCT), fluorescein angiography and indocyanine green angiography studies. These studies, however, were limited by low imaging resolutions and dye leakiness which precluded exact quantification of the microvascular network. The aim of this study is therefore to describe the vascular characteristics in the retina and choroid in different stages of STGD using double swept-source OCTA (dSS-OCTA) and to correlate them to the duration and stage of disease.

What are the new findings?

- Patients withSTGD reveal vascular changes in the retina and choriocapillaris in all disease stages. The avascular zone and the areas with rariefied flow signal in the different vascular plexuses increase with the duration and stage of disease, indicating progressive vascular decay most likely secondary to retinal pigment epithelium and neuronal loss. Furthermore, increased vascular damage is associated with decreased vision.

How might these results change the focus of research or clinical practice?

- OCTA enables improved visualization of the retinal and choriocapillary vasculature and is an important addition to the analysis of vascular damage in patients with STGD. The evaluation of retinal and choroidal vascular supply in STGD can have a significant impact on the individual prognosis and the optimal timing for possible therapeutic interventions.

INTRODUCTION

Stargardt disease (STGD) is the most common cause of hereditary juvenile macular dystrophy with a prevalence of about 1:10.000.[1] The disease mainly affects young patients (6–45 years) and causes a progressive, irreversible bilateral loss of central vision.[2] Fundus examination reveals a beaten bronze or a bull's-eye macular appearance and characteristic deep yellowish-white fish-shaped flecks in the macular and perimacular region. The end-stage fundus aspect is characterised

by extensive retinal pigment epithelium (RPE) and choriocapillaris (CC) atrophy, with resorbed flecks and sparse pigmentation.[3]

The underlying pathophysiology of STGD is not yet fully understood. It is generally accepted that mutations in the ABCA4 gene cause ATP-binding cassette (ABC) protein dysfunction, leading to malfunctioning photoreceptor cells and the deposition of lipofuscin in RPE cells.[4] The initial step of RPE damage is detectable in fundus autofluorescence (FAF) images, currently the standard diagnostic modality for STGD.[4] Other diagnostic tools such as optical coherence tomography (OCT), fluorescein angiography and indocyanine green angiography exhibit concomitant thinning and loss of the CC in STGD.[5]

Optical coherence tomography angiography (OCTA) is a non-invasive technique for imaging the microvasculature of the retina and choroid.[6] Few studies to date have analysed the retinal and choroidal vasculature in STGD using OCTA.[3 7 8] To the best of our knowledge, none of those studies analysed OCTA findings in different disease stages, or examined vascular changes in relation to the disease's duration.

The aim of this STGD cohort study is therefore to describe the vascular characteristics in the retina and choroid in different stages of STGD using double swept-source OCTA (dSS-OCTA) and to correlate them to the duration and stage of disease.

MATERIALS AND METHODS

Study design

This was a prospective, cross-sectional, monocentric, observational case–control study. All patients consulted our eye centre for the first time between 2000 and 2018 and were examined in the study between 2017 and 2018.

Inclusion and exclusion criteria

Patients with STGD and controls with relevant systemic disease like diabetes mellitus or cardiovascular diseases were excluded. Only patients with STGD with proven ABCA4 mutation and no other retinal diseases were included. Controls were only included when exhibiting no retinal or other ophthalmological diseases. Eyes revealing media opacities, such as an advanced cataract, were also excluded, due to reduced OCTA signal strength. Only images with signal strength equal to or greater than 7 were included. Furthermore, images with other artefacts like motion artefacts were excluded.

Ophthalmological examination

Patients underwent a comprehensive ophthalmological examination including measurement of best corrected visual acuity (BCVA in logMAR), assessment of intraocular pressure, fundus examination and FAF imaging (Spectralis HRA, Heidelberg, Germany). OCTA examination was performed using the Plex Elite OCTA system (Zeiss PLEX Elite 9000, Germany), which employs a full spectrum dSS-OCT (wavelength 1050 nm, A-scan rate 100.000 A-scans/s, A-scan depth 3.0 nm in tissue). 6×6 mm^2 and 9×9 mm^2 volume scans were performed.

Used OCTA slabs

The automated segmentation of the superficial capillary plexuses (SCP, slab from internal limiting membrane to inner plexiform layer), deep capillary plexuses (DCP, slab from inner plexiform layer to outer plexiform layer), the outer retina to choriocapillaris layer (ORCC, slab from outer plexiform layer to RPE) and the CC (slab 29–49 µm under the RPE) were obtained using the manufacturer's built-in software. Automatic segmentation was controlled and corrected by the investigators for misalignments.

Phenotypical classifications

Patients were clinically graded according to the Fishman STGD classification.[9] Stage (S) 1 is characterised by macular pigmentary changes and irregular pigmentary spots (flecks) located within one disc diameter of the fovea. S2 is identified when the pigmentary changes and pisciform flecks are located beyond the vascular arcades temporally and often extend nasally to the optic disc. S3 is defined by the resorption of previously diagnosed flecks resulting in focal CC and RPE atrophy of the macula. S4 is characterised by diffusely absorbed flecks and extensive CC and RPE atrophy throughout the entire central fundus.

Image analysis

To analyse vascular changes in different STGD stages, OCTA images were exported and analysed using a self-designed analysis tool programmed in language R (www.r-project.org). Two independent and masked investigators (MR, AG) quantified the foveal avascular zone (FAZ) in the SCP and DCP using a freehand selection tool (figure 1). The FAZ in the SCP and DCP in all STGD stages and controls were compared with each other. In

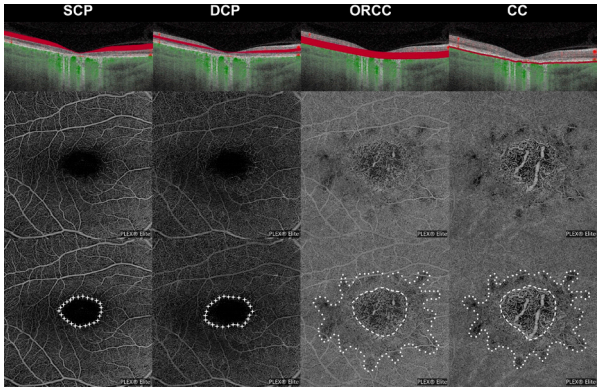

Figure 1 Analyses of vascular network. Detection of the avascular area in superficial and deep capillary plexuses (SCP and DCP; stars, lowest row), as well as detection of the area of rarfied optical coherence tomography angiography (OCTA) signal (points, lowest row) and complete atrophy (stripes, lowest row) in the outer retina to choriocapillaris (ORCC) layer and choriocapillaris (CC). Patient ID 19 (see table 1) is shown.

the ORCC and CC the area of rarefied flow and the area of complete vascular atrophy enabling a direct view of the choroid were determined and compared among the four disease stages (figure 2). If the area to be measured accommodated into the 6×6 mm^2 volume scan, that scan was preferred due to its higher resolution. As soon as the area to be measured exceeded the 6×6 mm^2 volume scan, the 9×9 mm^2 volume scan was used.

Patient and public involvement

This research was done without patient involvement. Patients were not invited to comment on the study design and were not consulted to develop patient-relevant outcomes or interpret the results. Patients were not invited to contribute to the writing or editing of this document for readability or accuracy.

Statistical analysis

SPSS V.20.0 was used for statistical analysis. For the linear mixed models R-package lmerTest was used. A probability (p) value of $\alpha<0.05$ was considered statistically significant. For descriptive data analysis, the mean and SD were calculated. The Mann-Whitney U test was used to compare patient characteristics. Bland-Altman plots and intraclass correlation coefficient (ICC) were used to determine the reproducibility and variability of the manual quantification in pixels of the FAZ in the SCP and DCP, as well as the area of rarefied flow and the area of complete vascular atrophy in the ORCC and the CC layer between the two examiners. A linear mixed model, using the diagnosis and stage of disease as a fixed factor and the patient ID as a random factor, was used to analyse differences in the FAZ in the SCP and DCP and in the area of ORCC and CC. We also included signal strength values for each image in the model. To reveal any association between the patient's age, disease duration and BCVA with vascular changes, we calculated the Spearman's r.

RESULTS

Study population

Twenty-three patients with STGD met all inclusion criteria. Twenty-three age-matched, healthy participants with a BCVA of 0.0 logMAR or better served as controls.

Patient characteristics

A total of 45 eyes of 23 patients with genetically secured STGD (13/10 females/males) were included. One eye was excluded due to artefacts and resulting partially reduced signal strength because of significant posterior polar cataract. The average age at initial diagnosis of the disease was 24.0 years (range 9–50) and 37.9 years (range 18–74) at the time of the study examination. Table 1 presents detailed information of our study group. Twenty-two eyes of 11 patients were assigned to Fishman STGD classification S1, 6 eyes of 3 patients to S2, 15 eyes of 8 patients to S3 and 2 eyes of 1 patient to S4. The age at disease onset was similar in all stages (S1: 24.8±12.8 years; S2: 14.7±6.0 years; S3: 27.5±9.5 years; S4: 14.0 years, p=0.32). However, patients in S3 and S4 were older than those in S1 and S2 at the time of the OCTA examination (S1: 33.1±10.8 years; S2: 21.3±2.9 years; S3: 48.9±15.5 years; S4: 52.0 years, p=0.01). Twenty-three controls (11/12 females/males, 23 eyes) with an average age of 37.1 years (range 20–69) were included. There was no significant difference in age between the STGD group and controls (p=0.97).

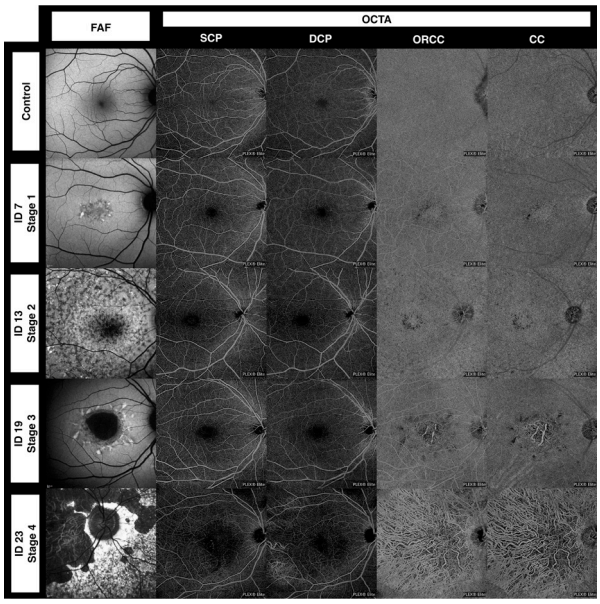

Figure 2 Optical coherence tomography angiography (OCTA) and fundus autofluorescence (FAF) imaging in a control patient (upper row) and four different stages of Stargardt disease based on the Fishman classification. For detailed information on these four patients, see table 1. CC, choriocapillaris; DCP, deep capillary plexus; ORCC, outer retina to choriocapillaris; SCP, superficial capillary plexus.

Qualitative analysis of the OCTA images in STGD

dSS-OCTA imaging yielded detailed images of the retinal microcirculation and a homogeneous texture of the ORCC and CC flow signal with a dense and fine granular appearance in all control patients (figure 2). All patients with STGD, in contrast, exhibited structural vascular changes with rarefied or even totally absent flow signal in SCP, DCP, ORCC and CC (figure 2). These structural changes were subtle in S1 and S2 and most pronounced in S3 and S4. Rarefied flow in the ORCC and CC was observed in all 45 eyes (100%) while ORCC and CC atrophy was detected in 25 of 45 eyes (53%) of patients with STGD. Concomitant rarefication and atrophy of the CC was detected in 4 of 22 eyes (18%) in S1, in 4 of 6 eyes (67%) in S2, in all 15 eyes (100%) in S3 and in both eyes (100%) in S4.

Quantitative OCTA analysis of OCTA images in STGD

To quantitatively assess the described vascular alterations, OCTA images of the SCP, DCP, ORCC and CC were analysed by two independent and masked examiners as described above. Bland-Altman plots (figure 3) reveal

Table 1 Clinical and molecular data on the patients with STGD in our study group

ID	Age (years)	Onset (years)	Sex	BCVA OD logMAR	BCVA OS logMAR	Fishman STGD classification	Mutation 1	Mutation 2	Mutation 3
1*	40	10	F	2	2	1	c.5196+2T>C (Splice)	c.5882G>A (p.Gly1961Glu)	
2	23	15	F	2	2	1	c.2041C>T (p.Arg681Xaa (het.))	c.5882G>A (p.Gly1961Glu)	
3	23	17	F	1.3	1	1	c.1622T>C (p.Leu541Pro)	c.3113C>T (p.Ala1038Val)	c.5882G>A (p.Gly1961Glu)
4	27	23	M	1	1	1	c.4462T>C (p.Cys1488Arg)	c.5882G>A (p.Gly1961Glu)	
5	28	24	F	1	1	1	c.2588G>C (p.Gly863Ala, Splice)	c.2828G>A (p.Arg943Gln)	c.5603A>T (p.Asn1868Ile)
6	39	31	M	1.3	1	1	c.5461-10T>C (Unknown)	c.5882G>A (p.Gly1961Glu)	
7	37	36	F	0.3	0.1	1	c.3322C>T (p.Arg1108Cys)	c.5882G>A (pGly1961Glu)	
8	52	42	F	1	1	1	c.2894A>G (p.Asn965Ser)	c.5882G>A (p.Gly1961Glu)	
9	49	48	M	0.3	0.1	1	c.2588G>C (p.Gly863Ala)	c.2588G>C (p.Gly863Ala)	
10	22	13	M	1	1	1	c.3322C>T (p.Arg1108Cys)	c.5882G>A (p.Gly1961Ala)	
11	25	14	M	1	1	1	c.5882G>A (p.Gly1961Glu)	c.6238_6239delTC (p.Ser2080HisfsX16)	
12†	18	9	M	1.3	1	2	c.2588G>C (p.Gly863Ala, Splice)	c.6238_6239delTC (p.Ser2080HisfsX16)	
13†	23	14	F	1.3	1.3	2	c.2588G>C (p.Gly863Ala, Splice)	c.6238_6239delTC (p.Ser2080HisfsX16)	
14	23	21	M	0.6	0.6	2	c.2588G>C (p.Gly863Ala, Splice)	c.858+2T>A (Unknown)	
15	28	19	F	2	2	3	c.1622T>C (p.Leu541Pro)	c.3113C>T (p.Ala1038Val)	
16*	51	22	M	1.2	1.1	3	c.5196+2T>C (Splice)	c.5882G>A (p.Gly1961Glu)	
17	40	23	F	0.9	0.9	3	c.5413A>G (p.Asn1805Asp)	c.5714+5G>A (Unknown)	
18*	57	27	F	0.9	0.8	3	c.5196+2T>C (Splice)	c.5882G>A (p.Gly1961Glu)	
19	74	27	M	1.3	1.3	3	c.5882G>A (p.Gly1961Glu)	Deletion exon 18–19	
20	30	27	M	1.3	1.3	3	c.1622T>C (p.Leu541Pro)	c.3113C>T (p.Ala1038Val)	
21	52	25	F	1.3	1.3	3	c.2692G>T (p.Glu898Xaa)	c.5461-10T>C (Unknown)	c.5606C>T (p.Pro1869Leu)
22	59	50	F	−0.1	0.1	3	c.4610C>T (Unknown)	c.5461-10T>C (Unknown)	
23	52	14	F	2.3	2.3	4	c.2931G>A (p.Gly978Ser)	c.5714+5G>A (Unknown)	

*Siblings.
†Siblings.
BCVA, best corrected visual acuity; F/M, female/male; OD, right eye (oculus dexter); OS, left eye (oculus sinister); STGD, Stargardt disease.

strong inter-rater reliability between the two examiners concerning their analyses of the avascular area in the SCP and DCP, the area of rarefied and absent flow in the ORCC and CC. The ICC for the avascular area in the SCP was 0.99 (p<0.0001), respectively 0.99 (p<0.0001) in the DCP, 0.99 (p<0.0001) and 0.99 (p<0.0001) regarding the area of rarefied flow and 1.0 (p<0.0001) and 1.0 (p<0.0001) regarding the area of absent flow in the ORCC and the CC layer. Relying on such minimal interobserver variability, we employed one grader's (MR) quantification for the analyses below.

Analysis of the retinal vasculature

All patients with STGD revealed an enlarged FAZ in the SCP compared with controls which expanded as the disease stage increased (S1: 0.21±0.10 mm^2; S2:

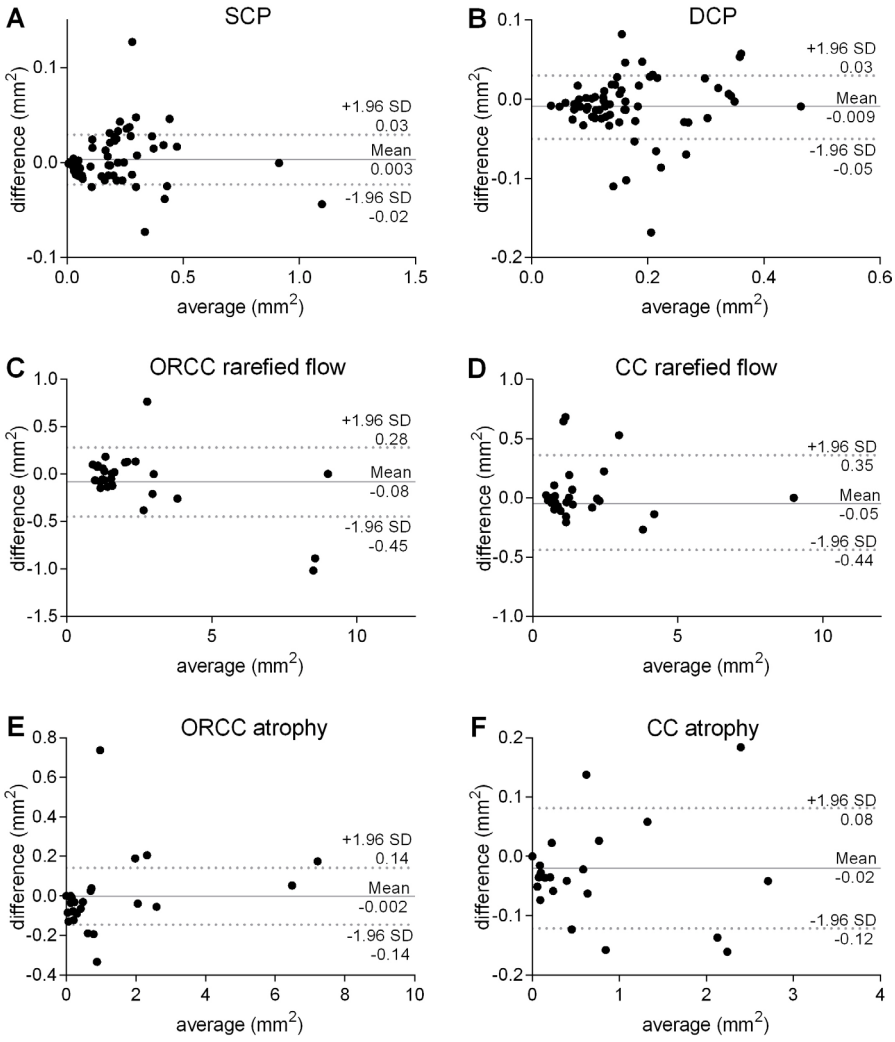

Figure 3 Bland-Altman analysis of inter-rater reliability. Two independent and masked investigators (MR, AG) quantified the foveal avascular zone (FAZ) in the superficial capillary plexus (SCP, A) and deep capillary plexus (DCP, B) using a freehand selection tool. Furthermore, the area of rarefied flow and complete atrophy was quantified in the outer retina to choriocapillaris (ORCC, C and E) and the choriocapillaris (CC, D and F) layer.

0.23±0.03 mm^2; S3: 0.27±0.14 mm^2; S4: 0.99±0.12 mm^2; controls: 0.03±0.01 mm^2, over all p<0.01, figure 4A1). Similarly, the FAZ in the DCP was enlarged in S1, S2, S3 and S4 compared with controls (S1: 0.16±0.09 mm^2; S2: 0.17±0.04 mm^2; S3: 0.21±0.11 mm^2; S4: 0.40±0.08 mm^2; controls: 0.11±0.03 mm^2, over all p<0.01, figure 4A2). Furthermore, patients with STGD revealed a larger FAZ in the SCP compared with DCP (0.26±0.19 mm^2 vs 0.19±0.10 mm^2, figure 4A3). In contrast, our controls exhibited a smaller FAZ in the SCP compared with DCP (0.03±0.01 mm^2 vs 0.11±0.03 mm^2, figure 4A3).

Analysis of the choroidal vasculature

Similar to the retinal vasculature findings, altered OCTA signals in ORCC and CC increased with advancing STGD stages. The area of rarefied OCTA signal in the ORCC was increased in S2, S3 and S4 compared with S1 (S1: 1.56±0.58 mm^2; S2: 8.69±0.75 mm^2; S3: 7.69±2.41 mm^2; S4: 9.00±0 mm^2; over all p<0.01, figure 4B1). Similarly, the area of rarefied flow in the CC was increased in S2, S3 and S4 when compared with S1 (S1: 1.07±0.46 mm^2, S2: 8.46±0.86 mm^2; S3: 7.05±2.88 mm^2; S4: 9.00±0 mm^2; over all p<0.01, figure 4B2). Interestingly, the area of rarefied flow in the ORCC (2.38±2.03 mm^2) was larger than the one in the CC layer (1.86±1.80 mm^2) in all patients with STGD independent of disease stage (figure 4B3).

Finally, the area of vascular atrophy in the ORCC also grew with increasing stage and was larger in S4 than in S1, S2 and S3 (S4: 6.90±0.58 mm^2; S1: 0.03±0.07 mm^2; S2: 0.08±0.07 mm^2, S3: 0.99±0.88 mm^2, over all p<0.01, figure 4C1). Similarly, the area of vascular atrophy in the CC grew with increasing stage and was increased in S4 compared with S1, S2 and S3 (S4: 6.69±0.79 mm^2; S1: 0.03±0.07 mm^2; S2: 0.05±0.04 mm^2; S3: 1.01±0.90 mm^2, over all p<0.05, figure 4C2). The area of atrophy in the ORCC (1.31±1.89 mm^2) was similar to the one in the CC layer (1.18±1.82 mm^2) in all patients with STGD independent of disease stage (figure 4C3).

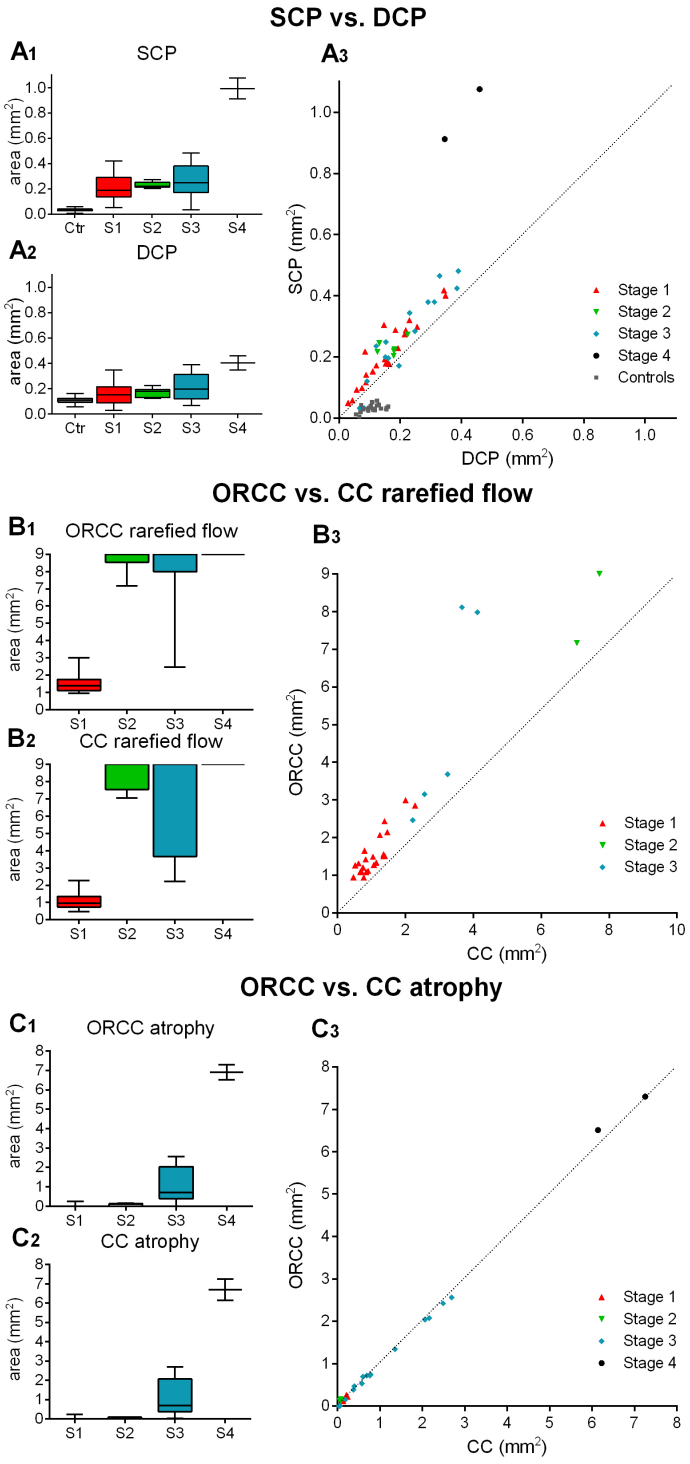

Figure 4 Quantitative evaluation of vascular alterations in Stargardt disease (STGD). Box and whiskers plot demonstrating the area of vascular alterations (in mm^2) of patients in different stages of STGD (S1–S4) and controls (Ctr). Data on the foveal avascular zone in the superficial and deep capillary plexuses (SCP and DCP) are depicted in A1–A3, data on the area of rarefication of flow signal/atrophy in the outer retina to choriocapillaris (ORCC) layer and choriocapillaris (CC) are shown in B1–B3 and C1–C3, respectively. To assess any correlation between the areas of rarefied flow in the ORCC compared with the CC layer, we excluded data of 17 eyes as the area of rarefied flow exceeded the maximum available image size of 9×9 mm^2. A linear mixed model, using the diagnosis and stage of disease as a fixed factor and the patient ID as a random factor, also including signal strength values for each image, was used to analyse differences between the groups. All analyses (A1, A2, B1, B2, C1, C2) show a significance value of $p<0.01$.

Correlation between vascular alterations and patient's age, disease duration and BCVA

No association between patient age and the FAZ in the SCP (r=0.06, p=0.66) or the DCP (r=0.01, p=0.95) was revealed. Similarly, no significant correlation between patient age and the area of flow rarefication in the ORCC

(r=0.15, p=0.33) and the CC (r=0.16, p=0.30) was identified. However, patient age associated significantly with an enlarged area of atrophy in the ORCC (r=0.30, p=0.048) and the CC layer (r=0.34, p=0.02).

Furthermore, disease duration correlated with an enlarged FAZ in the SCP (r=0.42, p<0.01) and the DCP (r=0.39, p<0.01), as well as with an enlarged rarefied

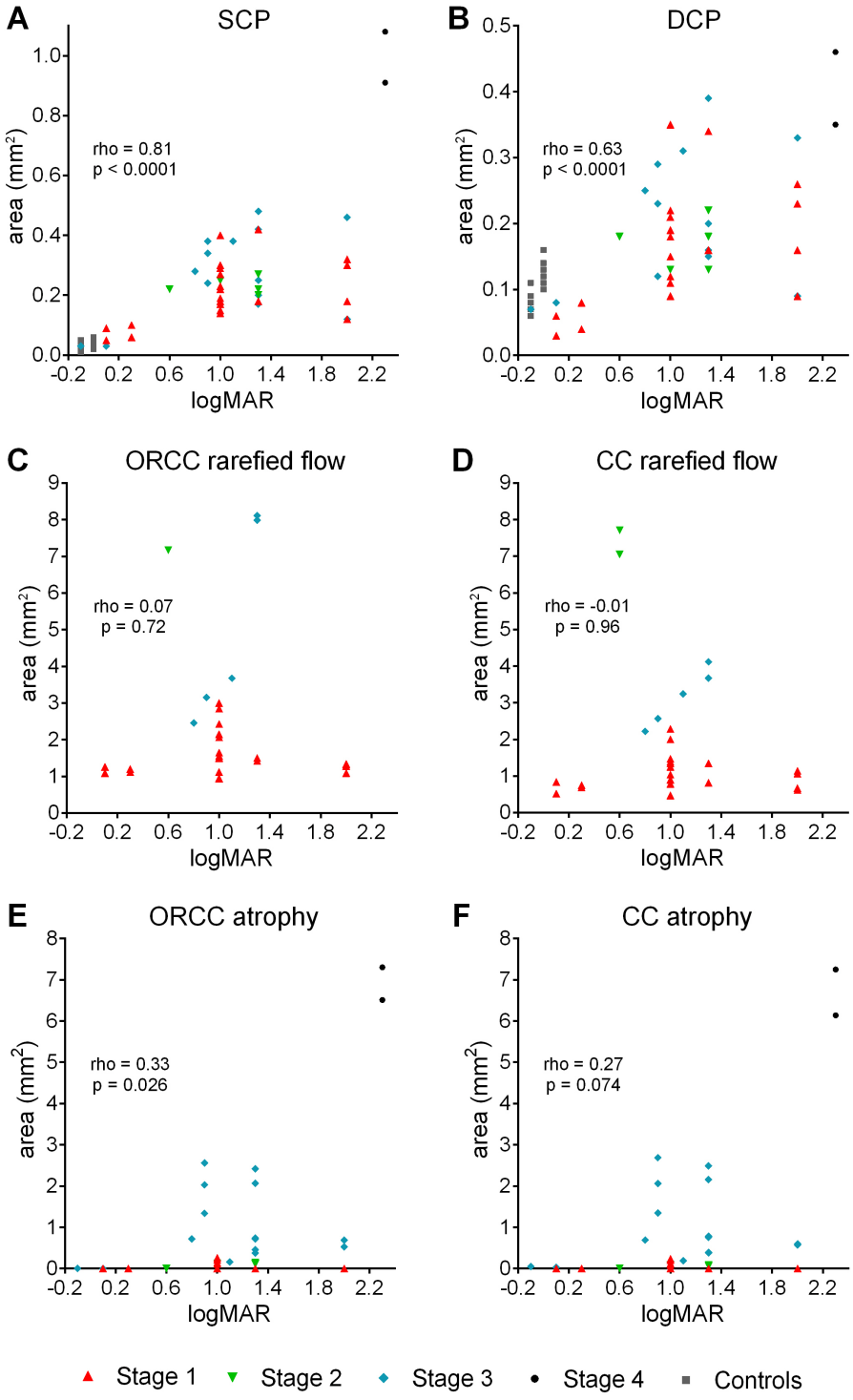

Figure 5 Association between best corrected visual acuity (BCVA) and vascular changes. Illustrated is the correlation between BCVA (in logMAR) and the foveal avascular zone (FAZ) in the superficial capillary plexus (SCP, A) and deep capillary plexus (DCP, B) and the areas presenting rarefied flow (C, D) and complete vascular atrophy (E, F) in the outer retina to choriocapillaris (ORCC) and choriocapillaris (CC). To assess any correlation between BCVA and the area of rarefied flow in the ORCC, respectively the CC layer, we excluded data of 17 eyes, respectively 16 eyes, as the area of rarefied flow exceeded the maximum available image size of 9×9 mm^2.

and atrophic area in the ORCC (r=0.37, p=0.01/r=0.66, p<0.001) and CC layer (r=0.40, p<0.01/r=0.67, p<0.001).

BCVA correlated negatively with the extent of the enlarged FAZ in the SCP (r=0.81, p<0.0001, figure 5A) and DCP (r=0.63, p<0.0001, figure 5B) in patients with STGD and controls, as well as with enlarged atrophic area in the ORCC (r=0.33, p=0.026, figure 5E) and a trend of enlarged atrophic area in the CC layer (r=0.27, p=0.074, figure 5F) in patients with STGD. We detected no significant correlation between BCVA and enlarged rarefied area in the ORCC and CC layer (r=0.07, p=0.72, figure 5C/r=−0.01, p=0.96, figure 5D).

DISCUSSION

To identify vascular alterations in STGD is an important prerequisite for defining disease pathophysiology, individual prognosis and the optimal time point for therapeutic interventions in the future. However, little is known about the microvascular alterations associated with STGD. Former studies using fluorescein or indocyanine green angiography already detected vascular changes in STGD.[5 10] These studies, however, were limited by low imaging resolutions and dye leakiness which precluded exact quantification of the microvascular network. The advent of OCTA has enabled in-depth imaging and analysis of the retinal and choroidal vasculature in chorioretinal disease.[6] The present study aimed to characterise vascular changes in STGD using dSS-OCTA. All our patients with STGD exhibited vascular alterations in the retina and choroidea that increased with age and disease stage, indicating progressive vascular decay over the disease course. Furthermore, increased vascular damage seems to be associated with decreased vision.

Few investigations have examined the retinal and choroidal vasculature in patients with STGD using OCTA.[3 7 11] Mastropasqua *et al* assessed the CC in 12 patients with STGD using OCTA and detected an extensive loss of the CC in areas of RPE atrophy.[11] Guduru *et al* quantitatively assessed the CC in STGD and demonstrated that the RPE loss was more pronounced than the concomitant CC loss indicating primary RPE degeneration followed by vascular atrophy.[7] Both studies, however, were limited by the use of spectral domain OCTA (SD-OCTA) technology, which is prone to image artefacts when assessing the choroidal vasculature.[6] To overcome this limitation, we employed dSS-OCTA, as it delivers more accurate imaging of the CC thanks to its longer wavelength and better sensitivity roll-off.[12 13] We distinguished two different CC textures in STGD: a central area of complete CC atrophy which permitted direct visualisation of deep choroidal vessels and a surrounding area of rarefied CC. These data support fluorescein angiography findings demonstrating a progressively hyperfluorescence in the borders of the area of atrophy in STGD, while the centre was isohypofluorescent.[10] While all patients with STGD revealed areas of rarefied CC in our study, areas of CC atrophy were predominantly found in more advanced STGD stages. In line with this observation, we detected a positive correlation between the time since first diagnosis and the area of CC atrophy, indicating progressive vascular decay in the CC layer. Prospective studies entailing longitudinal follow-up are warranted to clarify whether the areas of CC rarefication eventually become atrophic, and whether they precede or follow RPE atrophy during the disease course.

To the best of our knowledge, the ORCC layer has not been examined in STGD so far. Hitherto this layer has mainly been used to visualise features of type I and type II choroidal neovascularization (CNV).[14 15] The ORCC slab includes parts of the outer retina, the RPE and, to a small degree, the CC, and reveals a homogeneous architecture in healthy individuals. Patients with STGD, however, exhibit an ORCC slab emitting irregular and rarefied OCTA signals, and areas revealing a total loss of retinal signal texture with uncovered large-callipered vessels which increase with duration and stage of disease. Although recent studies indicate that SS-OCTA is capable of delivering ORCC angiograms with better image quality than SD-OCTA,[16] the projection artefacts from the inner retinal vessels (reduced in density in STGD) cannot be completely ruled out. Furthermore, shadowing artefacts from lipofuscin-containing flecks or window defects from atrophic RPE may enhance the area of alterations in the ORCC. Since the affected area in the ORCC was significantly larger than the SCP, DCP and CC, it is likely that a combination of the aforementioned phenomena contributes to the changes observed in the ORCC, and that the ORCC represents an overall measure to visualise retinal, RPE and choroidal anomalies in STGD.

While the choroidal vasculature has attracted the most interest,[8] considerably less is known about the retinal vasculature in STGD. Mastropasqua *et al* studied 12 patients with STGD and reported on a reduction in vessel density in the fovea within the SCP and DCP, a finding in line with ours.[11] In contrast to Battaglia Parodi *et al* who examined 19 patients with STGD,[3] our study revealed an enlarged FAZ in the SCP compared with the DCP, suggesting that the vascular damage is exacerbated in the inner retinal layers.[3] This discrepancy may be attributed to the older and more advanced cohort analysed in our study which may exhibit more pronounced vascular decay in the SCP secondary to neuronal loss. However, the small sample sizes of our study and the aforementioned studies preclude definitive conclusions. Further studies are needed to determine any differences between the SCP and DCP with confidence. Nevertheless, our study supports the aforementioned OCTA investigations revealing a reduced vascular density in the inner retina, and demonstrates that these vascular changes worsen with time and advancing disease stages. It is currently unknown whether the decay of the inner retinal vessels in STGD is a primary or secondary consequence of the weakening metabolic demand in the degenerating neuroretina. The hypothesis of primary regression of the vasculature with secondary loss of neurons, however, is unlikely since the ABCA4 gene is predominantly expressed in

photoreceptor cells[17] and only weakly in endothelial cells in the central nervous system.[18] Nevertheless, it is a possibility that cannot be entirely ruled out, and future studies are necessary to examine patients with STGD at a very early disease stage to prove or disprove that hypothesis. On the other hand, the vascular decay in the retina could be attributable to a reduced metabolic demand in the retina caused by progressing retinal degeneration. This hypothesis would be in line with findings demonstrating a correlation between macular vessel density and retinal atrophy[11] and would be supported by our study showing a correlation between the disease duration and vascular degeneration. In any case, the considerable vascular decay in the inner retina may constitute an important feature of STGD pathology and may specifically exacerbate the progressive degeneration of photoreceptors and inner retinal neurons over the disease course. This finding is particularly important in the context of promising therapeutic interventions such as gene therapy or stem cell transplantation, which need to be administered at an early disease stage or at least guided by the vascular pattern as visualised on OCTA.

We acknowledge that our analysis has limitations, including subjective classification of the type of disease and the absence of longitudinal follow-up. Due to our cohort's small size, the group size of the four different STGD stages varies between 2 and 22 eyes, which makes the classes harder to compare. Furthermore, our study enrolled only one patient presenting S4, which may have led to an overestimating or underestimating the OCTA findings at that stage. Using two eyes of a single patient might result in within-subject correlation. Nevertheless, since STGD is a rare disease, and although our cohort managed to attain a good size compared with previous studies,[3 7] sample size is still small. Therefore, we decided, as did other investigators,[3 7] to include both eyes of the patients with STGD in our study. We performed additional analyses only including the right eye of the patients. Due to smaller sample sizes, not all analyses that resulted in a significant level when using all eyes also reach significance when only using the right eye. Nevertheless, a trend toward significance becomes obvious in all our analyses (data not shown). Although carrying out multiple statistical tests in our study, we did not correct the p values due to small sample sizes. Therefore, some of the significant p values might be spurious. Furthermore, different dimensions of the OCTA scans may lead to different quantitative values.[19] Nevertheless, in view of the higher precision of the 6×6 mm^2 volume scan, we decided to prefer it, and it was only whenever the area to be measured exceeded the size of that scan that we opted to use the 9×9 mm^2 volume scan. Furthermore, since 9×9 mm^2 was the largest frame available, the areas of rarefied flow and atrophy in ORCC and CC may have been underestimated in some patients and therefore potential differences in eyes affected by large areas of rarefied flow and atrophy went undetected. Despite the existing body of evidence suggesting that the retinal plexuses merge at the edge of the FAZ, which may be thus considered a singular structure throughout the entire foveal thickness[20 21] and increased variability of measurements when assessing the FAZ size at different segments,[22] we chose to investigate the FAZ area separately in different retinal capillary plexuses (SCP and DCP) so as to compare our findings to the latest literature. As a result of choriocapillary atrophy, the large choroidal vessels are detected in the corresponding areas. Due to this limitation which prohibits a more objective measurement of, for example, perfusion density or vessel length density, we decided to manually detect the area of vascular changes/atrophy, as described before.[7] Nevertheless, a more objective means of detecting vascular changes would be desirable. To the best of our knowledge, however, there is no such analysis procedure available that does justice to the present situation of patients with STGD. In light of these limitations, further prospective studies offering increased power, improved OCTA imaging technology and longitudinal follow-up data are warranted to determine the vascular phenotype of STGD with confidence.

In summary, to the best of our knowledge this is the first and largest cohort-based study investigating vascular changes in different stages of STGD using dSS-OCTA technology, which enables improved visualisation of the deep retinal and choriocapillary layers and thus fewer image artefacts. Our study confirms the essential findings of previous studies using angiography or SD-OCTA and illustrates with more detail the considerable vascular alterations in all layers of the retina and choroid in STGD which increase with the disease's duration and advancing stage, indicating progressive vascular decay over the disease course. Furthermore, we demonstrated that increased vascular damage is associated with decreased vision. Further prospective and especially longitudinal OCTA studies are required to validate our results, which may have a significant impact on individual prognosis and the optimal timing for possible therapeutic interventions.

Acknowledgements MR is a recipient of a scholarship from the 'Dr Gabriele Lederle-Stiftung' and thanks this organisation for their support.

Contributors MR has conducted the acquisition of data, data analysis and interpretation, has made substantial contribution to conception and design of the manuscript and has been involved in drafting the manuscript. AG has conducted the data analysis, has made substantial contributions to acquisition of data and has been involved in drafting the manuscript. BC, SL, SK and LJ have made substantial contributions to acquisition of data, and have been involved in drafting the manuscript. DB has conducted the data and statistical analysis and has been involved in drafting the manuscript. WL and HTA have made substantial contributions to acquisition of data, and have been involved in revising the manuscript critically for important intellectual content. CL has made substantial contributions to analysis and interpretation of data and has been involved in revising the manuscript critically for important intellectual content. In addition, all authors have given final approval of the version to be published. Each author has participated sufficiently in the work to take public responsibility for appropriate portions of the content and agreed to be accountable for all aspects of the work in ensuring that questions related to the accuracy or integrity of any part of the work are appropriately investigated and resolved. All authors read and approved the final manuscript.

Funding The Plex Elite OCTA system (Zeiss PLEX Elite 9000, Germany) was loaned to our clinic by Zeiss. The article processing charge was funded by the German Research Foundation (DFG) and the University of Freiburg in the funding programme Open Access Publishing.

Competing interests None declared.

Patient consent for publication Not required.

Ethics approval The study was approved by our institutional ethics committee and adhered to the tenets of the Declaration of Helsinki. Informed written consent was obtained from all patients with STGD and all controls.

Provenance and peer review Not commissioned; externally peer reviewed.

Data availability statement Data are available upon request.

ORCID iD

Michael Reich http://orcid.org/0000-0002-9813-8483

REFERENCES

1 Lewis RA, Shroyer NF, Singh N, *et al*. Genotype/Phenotype analysis of a photoreceptor-specific ATP-binding cassette transporter gene, ABCR, in Stargardt disease. *Am J Hum Genet* 1999;64:422–34.10.1086/302251
2 Hadden OB, Gass JD. Fundus flavimaculatus and Stargardt's disease. *Am J Ophthalmol* 1976;82:527–39.
3 Battaglia Parodi M, Cicinelli MV, Rabiolo A, *et al*. Vascular abnormalities in patients with Stargardt disease assessed with optical coherence tomography angiography. *Br J Ophthalmol* 2017;101:780–5.
4 Molday RS. Insights into the molecular properties of ABCA4 and its role in the visual cycle and Stargardt disease. *Prog Mol Biol Transl Sci* 2015;134:415–31.
5 Giani A, Pellegrini M, Carini E, *et al*. The dark atrophy with indocyanine green angiography in Stargardt disease. *Invest Ophthalmol Vis Sci* 2012;53:3999–4004.
6 Koustenis A, Harris A, Gross J, *et al*. Optical coherence tomography angiography: an overview of the technology and an assessment of applications for clinical research. *Br J Ophthalmol* 2017;101:16–20.
7 Guduru A, Lupidi M, Gupta A, *et al*. Comparative analysis of autofluorescence and OCT angiography in Stargardt disease. *Br J Ophthalmol* 2018;102:1204–7.
8 Müller PL, Pfau M, Möller PT, *et al*. Choroidal flow signal in late-onset Stargardt disease and age-related macular degeneration: an OCT-Angiography study. *Invest Ophthalmol Vis Sci* 2018;59:AMD122–31.
9 Fishman GA. Fundus flavimaculatus. A clinical classification. *Arch Ophthalmol* 1976;94:2061–7.
10 Schwoerer J, Secrétan M, Zografos L, *et al*. Indocyanine green angiography in fundus flavimaculatus. *Ophthalmologica* 2000;214:240–5.
11 Mastropasqua R, Toto L, Borrelli E, *et al*. Optical coherence tomography angiography findings in Stargardt disease. *PLoS One* 2017;12:e0170343.
12 Adhi M, Liu JJ, Qavi AH, *et al*. Choroidal analysis in healthy eyes using swept-source optical coherence tomography compared to spectral domain optical coherence tomography. *Am J Ophthalmol* 2014;157:1272–81.
13 Xu J, Song S, Wei W, *et al*. Wide field and highly sensitive angiography based on optical coherence tomography with akinetic swept source. *Biomed Opt Express* 2017;8:420–35.
14 Roisman L, Zhang Q, Wang RK, *et al*. Optical coherence tomography angiography of asymptomatic neovascularization in intermediate age-related macular degeneration. *Ophthalmology* 2016;123:1309–19.
15 Miere A, Oubraham H, Amoroso F, *et al*. Optical coherence tomography angiography to distinguish changes of choroidal neovascularization after anti-VEGF therapy: monthly loading dose versus pro re NatA regimen. *J Ophthalmol* 2018;2018:1–7.
16 Miller AR, Roisman L, Zhang Q, *et al*. Comparison between spectral-domain and Swept-Source optical coherence tomography angiographic imaging of choroidal neovascularization. *Invest Ophthalmol Vis Sci* 2017;58:1499–505.
17 Tsybovsky Y, Molday RS, Palczewski K. The ATP-binding cassette transporter ABCA4: structural and functional properties and role in retinal disease. *Adv Exp Med Biol* 2010;703:105–25.
18 Warren MS, Zerangue N, Woodford K, *et al*. Comparative gene expression profiles of ABC transporters in brain microvessel endothelial cells and brain in five species including human. *Pharmacological Research* 2009;59:404–13.
19 Rabiolo A, Gelormini F, Marchese A, *et al*. Macular perfusion parameters in different Angiocube sizes: does the size matter in quantitative optical coherence tomography angiography? *Invest Ophthalmol Vis Sci* 2018;59:231–7.
20 Borrelli E, Sadda SR, Uji A, *et al*. Pearls and pitfalls of optical coherence tomography angiography imaging: a review. *Ophthalmol Ther* 2019;8:215–26.
21 Gariano RF, Iruela-Arispe ML, Hendrickson AE. Vascular development in primate retina: comparison of laminar plexus formation in monkey and human. *Invest Ophthalmol Vis Sci* 1994;35:3442–55.
22 Coscas F, Sellam A, Glacet-Bernard A, *et al*. Normative data for vascular density in superficial and deep capillary plexuses of healthy adults assessed by optical coherence tomography angiography. *Invest Ophthalmol Vis Sci* 2016;57.